

Article

# Methanation of CO<sub>2</sub> over Cobalt-Lanthanide Aerogels: Effect of Calcination Temperature

Joaquim Badalo Branco , Ricardo Pinto da Silva and Ana Cristina Ferreira \* 

Centro de Ciências e Tecnologias Nucleares and Centro de Química Estrutural, Instituto Superior Técnico, Universidade de Lisboa, Campus Tecnológico e Nuclear, Estrada Nacional 10, ao km 139.7, 2696-066 Bobadela, Portugal; jbranco@ctn.tecnico.ulisboa.pt (J.B.B.); ricardos7055@gmail.com (R.P.d.S.)

\* Correspondence: acferreira@ctn.tecnico.ulisboa.pt; Tel.: +351-21-994-6218

Received: 1 May 2020; Accepted: 20 June 2020; Published: 23 June 2020



**Abstract:** High surface area cobalt-lanthanide bimetallic aerogels were successfully synthesized by the epoxide addition method. The bimetallic aerogels were calcined at two different temperatures and either bimetallic oxides containing oxychlorides, Co<sub>3</sub>O<sub>4</sub>.3LnOCl (Ln = La, Sm, Gd, Dy and Yb) or perovskites, LnCoO<sub>3</sub> (Ln = La, Sm, Gd and Dy) were obtained at 500 or 900 °C, respectively. The exceptions are the aerogels of cerium and ytterbium, which after oxidation at 500 and 900 °C, stabilize as sesquioxides: Co<sub>3</sub>O<sub>4</sub>.3CeO<sub>2</sub> and 2Co<sub>3</sub>O<sub>4</sub>.3Yb<sub>2</sub>O<sub>3</sub>, the first at both temperatures and the second only at the highest temperature. The bimetallic cobalt-lanthanide oxychlorides or perovskites were tested as catalysts for the methanation of CO<sub>2</sub>. The cobalt catalytic activity is determined by the type and acid-base properties of the lanthanide oxide phase and by its pre-reduction under hydrogen. The best results were those obtained over the calcined aerogels pre-reduced under hydrogen. In particular, the highest values were those obtained over the Co-Ce aerogel calcined at 900 °C that in the same conditions present an activity comparable to that measured over a 5 wt.% Rh catalyst supported on alumina, one of the literature references. The activity and the selectivity increase with the catalysts' basicity, showing an inverse dependence of the reduction temperature that decreases along the lanthanide series either for the aerogels calcined at 500 or 900 °C. In general, the basicity of the aerogels calcined at 900 °C (perovskites) is higher and they are more active but less selective than those calcined at 500 °C (oxychlorides), which to our knowledge is for the first time reported for the methanation of CO<sub>2</sub>.

**Keywords:** methane; carbon dioxide; cobalt-4f element aerogels; bimetallic oxides

## 1. Introduction

Increasing consumption of fossil fuels has led to a considerable increase in the concentration of CO<sub>2</sub> in the atmosphere. Thus, climate change caused by greenhouse gases, in particular CO<sub>2</sub>, has become a huge problem and a major challenge at the same time [1]. In order to overcome this problem and turn it into an opportunity, three strategies have been developed: CO<sub>2</sub> emission control; capture and storage, and chemical transformation into value-added products. Carbon capture and storage (CCS) is important for achieving a rapid reduction in the concentration of CO<sub>2</sub> in the atmosphere but has some important disadvantages, in particular the high cost associated with its liquid transport or the high risk of leakage from geological formations where it is stored [1–3]. Therefore, the use of CO<sub>2</sub> as raw material and its transformation into value-added products is probably the best option.

Hydrogenation of CO<sub>2</sub> with hydrogen from renewable sources is an attractive path for chemical and fuel production that can not only reduce CO<sub>2</sub> emissions but can also respond to the growing demand and future shortage of fossil fuels. The main chemicals that can be obtained from CO<sub>2</sub> are alcohols and hydrocarbons, with particular emphasis on methane (power to gas technology) [4].

Typically, catalysts used to produce methane from CO<sub>2</sub> contain noble metals, nickel, cobalt supported on zeolites, carbon, silica, or alumina [5]. Noble metal-based catalysts, for example rhodium and ruthenium, are normally the best, producing almost exclusively methane, with CO<sub>2</sub> conversions in the range of 70–80% [6]. However, their high price makes them unattractive for commercial implementation. Nickel-based catalysts are often studied as alternative to noble metals because they have also a high activity and selectivity to methane. Iron and cobalt-based catalysts are mostly applied in the Fischer-Tropsch process (FT) to produce long chain hydrocarbons using syngas as reagent and the correlation between CO and CO<sub>2</sub> inspired researchers to study Fe and Co-based catalysts also for the hydrogenation of CO<sub>2</sub>. However, only cobalt-based catalysts are only reasonably active and selective for the production of methane but practically inactive for the production of higher chain hydrocarbons at atmospheric pressure from CO<sub>2</sub> [7,8].

The use of *f*-block elements as promoters for the hydrogenation of CO<sub>2</sub> has been also studied, in particular the use of additives containing cerium. Recent studies show that the addition of cerium to a Fe-Zr-K catalyst promotes the catalyst basicity, its reduction, the dispersion of active iron species and the activation of CO<sub>2</sub> [9]. In the case of cobalt catalysts, the addition of rare earths favors the reduction and dispersion of the metal and promotes an increase in selectivity to long chain hydrocarbons, namely C<sub>5+</sub> [10]. In particular, the addition of cerium to cobalt catalyst increases the specific surface area and the reduction of particle size, which promotes their catalytic activity [11,12].

The synthesis and study as catalysts of bimetallic oxides, in particular, those containing 4*f* or 5*f* block elements, nickel, copper, or calcium are current objectives of our laboratory. The results obtained up to now show that they are good catalysts for the production of syngas (partial oxidation of methane using O<sub>2</sub> as oxidant) [13–16], production of C<sub>2</sub> hydrocarbons using nitrous oxide as oxidant (ethane, ethylene) [17,18], and for the methanation of CO<sub>2</sub> [19,20]. They are also very stable, which is an advantage, in particular for nickel-based catalysts and their high activity was attributed to the existence of a synergism between the metals (Ni, Cu, Ca) and the *f*-block element that improve nickel activity and the catalysts stability [13,20].

In this article, we report the preparation of cobalt-lanthanide aerogels and their evaluation as catalytic precursors for the methanation of CO<sub>2</sub>. They were prepared by the sol-gel methodology (epoxide addition method), combining cobalt and six lanthanides (lanthanum, cerium, samarium, gadolinium, dysprosium, and ytterbium) and calcined at two different temperatures, which together with cobalt oxide provides two different types of lanthanide oxides and different contributions to their catalytic behavior. All catalysts were characterized by different techniques, e.g., XRD, SEM/EDS, BET, H<sub>2</sub>-TPR, CO<sub>2</sub>-TPD, and the catalytic tests were performed on a fix bed reactor at atmospheric pressure. The results were compared to those obtained in the same conditions over two reference catalysts, one commercial (Aldrich; 5 wt.% Rh/Al<sub>2</sub>O<sub>3</sub>) [5] and other from the literature (NiO/CeO<sub>2</sub>), that demonstrated to have a very good catalytic performance for the methanation of CO<sub>2</sub> [21].

## 2. Results and Discussion

### 2.1. Catalysts Characterization

The images obtained by SEM show that the cobalt-lanthanide aerogels have a morphology that depends on the calcination temperature. In the case of the aerogels calcined at 500 °C, their structure is spongy and composed of irregular spherical shape particles, while those calcined at 900 °C are composed of a regular shaped spherical nanoparticles agglomerates with an average size < 100 nm (Figure 1). The SEM images shown in Figure 1 are representative of the morphologies visualized for the remaining cobalt-lanthanide catalysts (Figures S1 and S2). EDS analysis at different points in each sample shows the different elements well distributed across the surface, a cobalt/lanthanide ratio very close to the expected value (1:1) and a cobalt mass percentage that is roughly the same for all catalysts regardless the calcination temperature, 24 ± 2% (Tables S2 and S3).

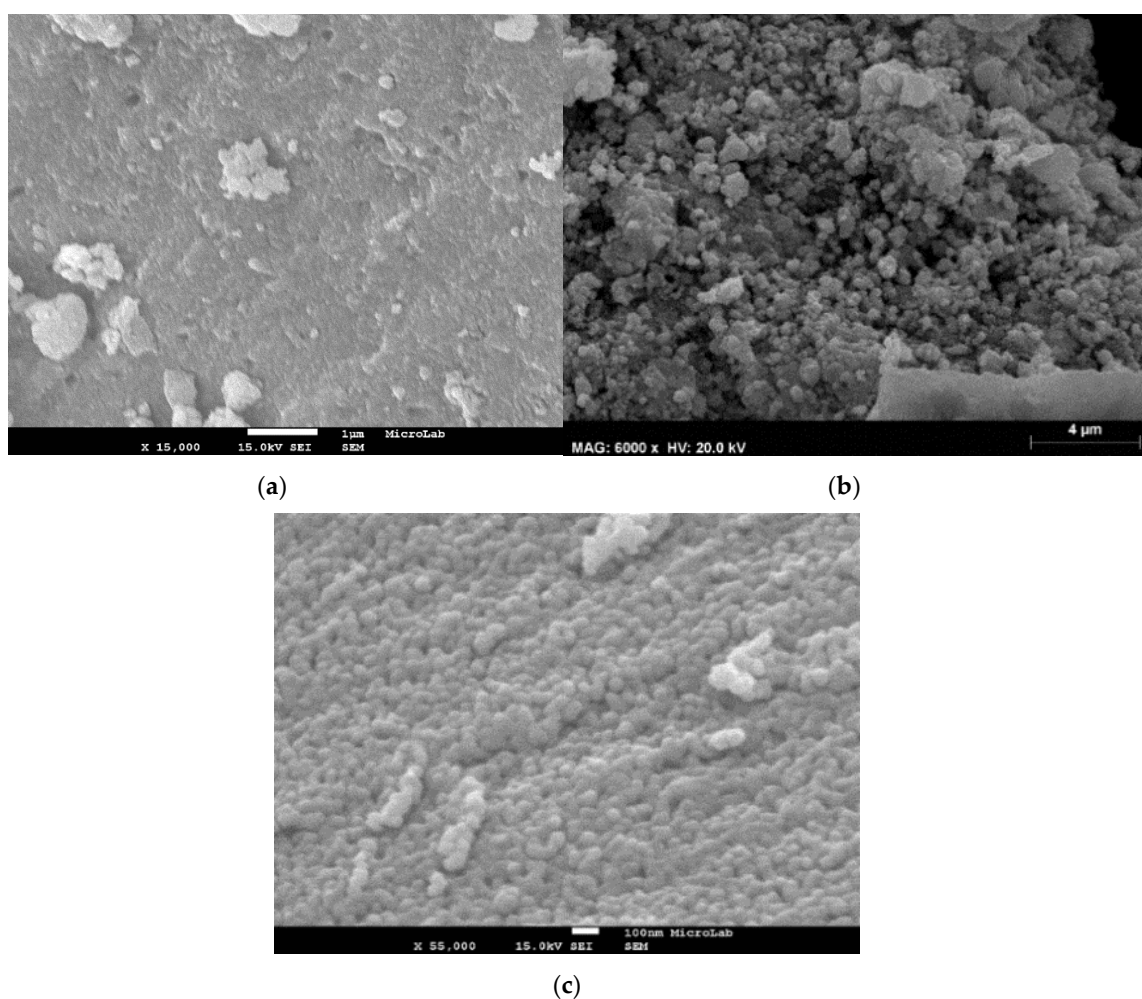


**Figure 1.** SEM images of the bimetallic Co-Ln oxides (1:1): (a) Co-Ce aerogel without calcination treatment ( $\times 15,000$ ); (b) Co-La aerogel calcined at  $500\text{ }^{\circ}\text{C}$  ( $\times 6000$ ) and (c) Co-Dy aerogel calcined at  $900\text{ }^{\circ}\text{C}$  ( $\times 55,000$ ).

X-ray diffraction data show that the cobalt-lanthanide aerogels calcined at  $500\text{ }^{\circ}\text{C}$  present, as expected, a low crystallinity (almost amorphous). Nevertheless, it was possible to identify cobalt oxide ( $\text{Co}_3\text{O}_4$ , cubic phase) in all samples, as well as cerium oxide ( $\text{CeO}_2$ ) in the case of the Co-Ce catalyst and lanthanide oxychlorides ( $\text{LnOCl}$ ; Ln = La, Sm, Gd; tetragonal phases) in the case of the remaining catalysts. The exceptions were the dysprosium and ytterbium calcined aerogels where only the patterns of cobalt oxide phase were observed (Figure 2a). It is known that lanthanides, particularly those from the beginning of the series, tend to form oxychlorides when chlorine salts are used as starting reagents [22]. The formation of lanthanide oxychlorides is thermodynamically favorable at low temperatures, while the formation of perovskites or sesquioxides becomes preponderant at higher temperatures ( $>650\text{ }^{\circ}\text{C}$ ), except for the cerium chloride system since the formation of  $\text{CeO}_2$  is thermodynamically favored at lower temperatures ( $T > 200\text{ }^{\circ}\text{C}$ ) [23].

This temperature effect was confirmed by the XRD patterns obtained for the cobalt-lanthanide aerogels calcined at  $900\text{ }^{\circ}\text{C}$  that shows the formation of perovskites ( $\text{LnCoO}_3$ , Ln = La, Sm, Gd, and Dy, hexagonal for La and orthorhombic for the other elements), except for the cerium and ytterbium catalysts. If the first is the known exception, the formation of  $\text{YbCoO}_3$  requires oxidation temperatures above  $1100\text{ }^{\circ}\text{C}$ , much higher than that used in this work [24]. Relative to the cobalt particles' size, they were estimated by Scherrer's equation. In the case of aerogels calcined at  $500\text{ }^{\circ}\text{C}$ , the  $\text{Co}_3\text{O}_4$  particle size is around  $16 \pm 2\text{ nm}$ , expect for cobalt-cerium (23 nm). For aerogels calcined at  $900\text{ }^{\circ}\text{C}$ ,

the  $\text{Co}_3\text{O}_4$  particle size is 37 nm for the cerium and 48 nm for ytterbium catalysts and  $44 \pm 7$  nm for catalysts in perovskite phase (Table S4).

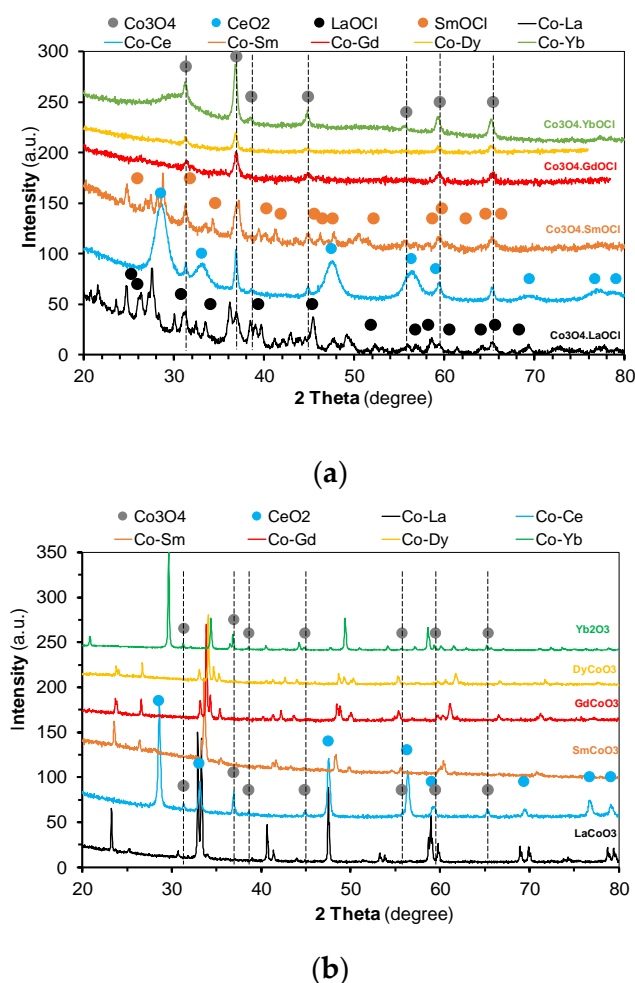


**Figure 2.** X-ray diffraction patterns of the Co-Ln aerogels calcined at: 500 °C (a) and 900 °C (b).

The X-ray patterns obtained after the catalytic studies with aerogels calcined at 500 °C show a partial reduction of  $\text{Co}_3\text{O}_4$  to  $\text{CoO}$  in the case of cerium and samarium catalysts (Figure 3a), while for the others, the reduction seems to be total ( $\text{Co}_3\text{O}_4$  to  $\text{Co}$ ) with the formation of metallic cobalt not detected by XRD (Figure 3a only shows the case of lanthanum), which could be explained by its crystallites due to being highly dispersed and having a low size. It is possible to observe that in most of the cases the metallic cobalt phase it is not observed/detected on XRD patterns, so it is difficult to estimate the particle size after catalytic reaction (Table S4). Of note, the stability of oxychlorides and cerium oxide between 250–450 °C, the range of temperatures used in this work catalytic studies. In the case of the aerogels calcined catalysts at 900 °C, the formation of metallic cobalt was only detected in the case of the ytterbium catalyst but due to the low crystallinity of the samples cannot be discard for the other cobalt-lanthanide bimetallic oxides, especially in the case of cerium. However, the main modification is the evolution of the rare earth oxide phase: perovskites ( $\text{LnCoO}_3$ ) are not stable and evolve to sesquioxides ( $\text{Ln}_2\text{O}_3$ ) (Figure 3b). So, clearly the calcined aerogels change during reaction and at steady state, the main active specie is cobalt together with lanthanide oxychlorides or lanthanide sesquioxides for samples calcined at 500 and 900 °C, respectively. In the case of aerogels calcined at 500 °C and subjected to a pre-reduction treatment under hydrogen, the only patterns observed before and after reaction are those of metallic cobalt and oxychlorides, whereas in the case of aerogels calcined at 900 °C, the only patterns observed before and after reaction are those of metallic cobalt and

sesquioxides (Figure 3c). In both cases, the exception is the Co-Ce bimetallic oxide where the only patterns observed are those of Co and CeO<sub>2</sub>. These results confirm our previous statement that cobalt together with lanthanide oxychlorides or lanthanide sesquioxides are the main active species present in the calcined aerogels, which was underlined by the pre-reduction treatment.

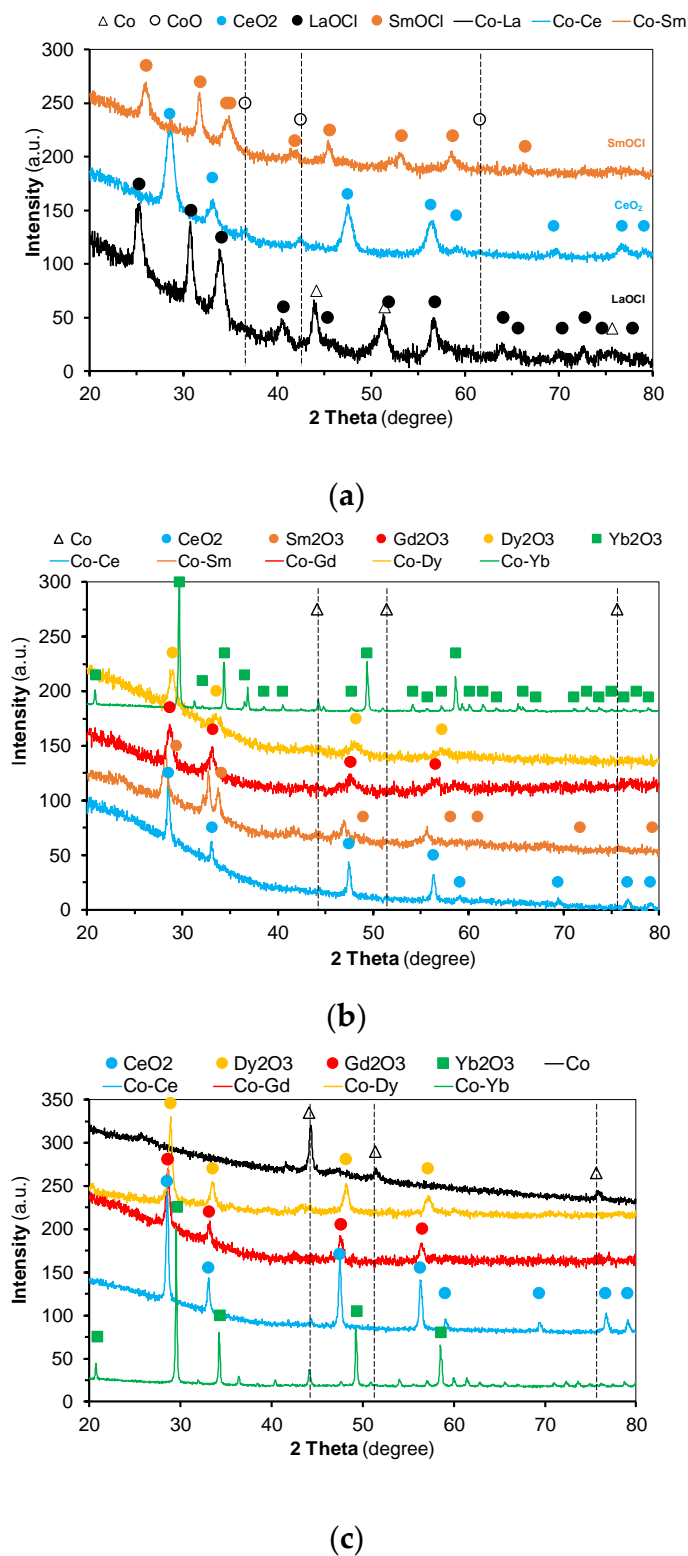


**Figure 3.** X-ray diffraction patterns obtained after reaction for the bimetallic oxides used as calcined at 500 °C (a) and 900 °C, without and with pre-reduction, (b) and (c), respectively.

The H<sub>2</sub>-TPR results confirm that each lanthanide has an effective influence on the cobalt bimetallic oxides oxygen's reducibility/lability and either for the aerogels calcined at 500 °C (Figure 4a) or those calcined at 900 °C (Figure 4b), the main reduction steps occur at temperatures well above the temperature recorded for the reduction of pure cobalt oxide, prepared by the same methodology and calcined also at 500 and 900 °C (temperatures at maximum reduction rate (T<sub>m</sub>) = 335 and 378 °C, respectively).

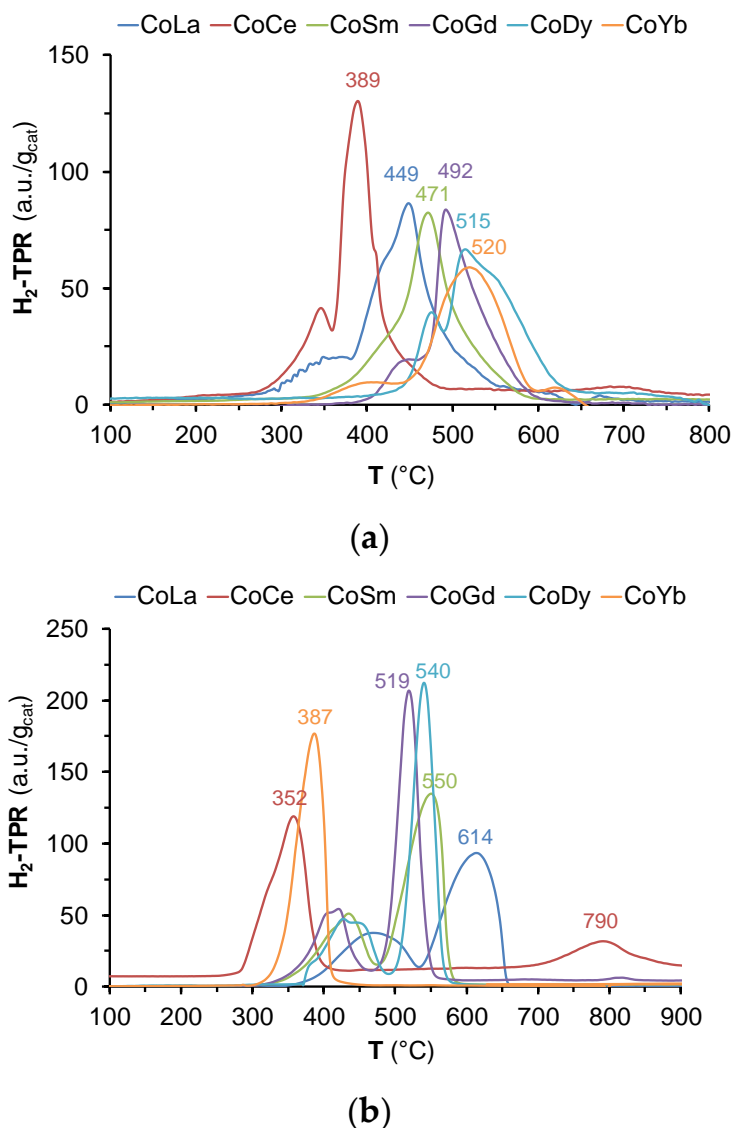
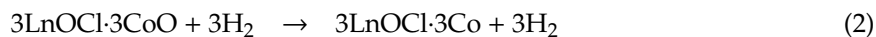
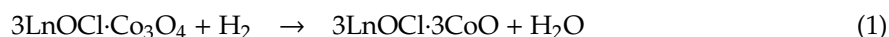


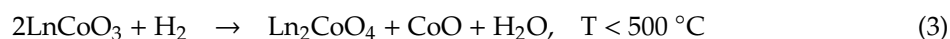
**Figure 4.** H<sub>2</sub>-TPR profiles for bimetallic cobalt-lanthanide oxides calcined at 500 °C (a) and 900 °C (b).

For the Co-Ln aerogels calcined at 500 °C that in addition to cobalt oxide have lanthanide oxychlorides in their composition (Ln = La, Sm, Gd, Dy, and Yb), the reduction profiles are complex but, in all cases, delimited by two peaks or shoulders. Taking into account the XRD analysis of the H<sub>2</sub>-TPR products that confirms the stability of the oxychlorides and the formation of metallic cobalt, these peaks can be attributed to the reduction of cobalt oxide in two stages (Equations (1) and (2)) and the presence of lanthanide oxychlorides seems to influence this reduction because the respective reduction temperatures increase throughout the series of lanthanides, except in the case of Co-Ce bimetallic oxide (T<sub>m</sub> = 389, 449, 471, 492, 515, 520 for Ln = Ce, La, Sm, Gd, Dy, Yb, respectively). It is important to note that we found an excellent correlation between the experimental and the theoretical

values for the consumption of hydrogen (Table S5), which confirms the expected global reduction mechanism (Equations (1) and (2)).



For the Co-Ln aerogels calcined at 900 °C, the H<sub>2</sub>-TPR profiles present also a better defined two-step reduction mechanism, the first step associated with the reduction of LnCoO<sub>3</sub> to Ln<sub>2</sub>CoO<sub>4</sub> and the second one with the reduction of CoO to metallic Co and formation of sesquioxides (Equations (3) and (4)) [25]. The experimental and expected values for hydrogen consumption correlate also very well (Table S6).



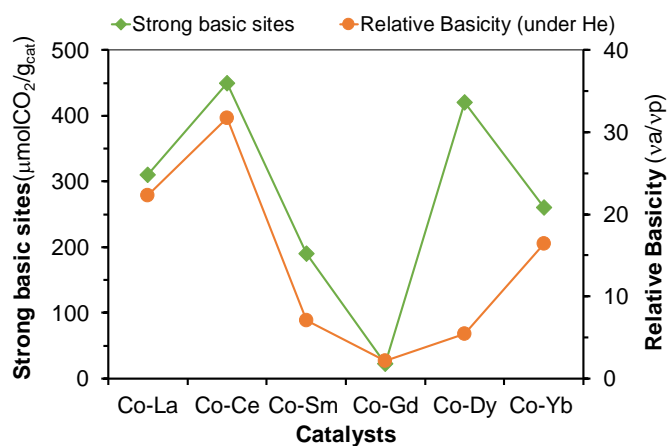
The T<sub>m</sub> reflects the stability of perovskites phases that decrease throughout the lanthanide series (T<sub>m</sub> = 614, 550, 540, 519, 398, 352 for Ln = La, Sm, Dy, Gd, Yb, Ce, respectively), which are higher and exactly the opposite of we have found for the aerogels calcined at 500 °C, except of cerium follows the data known from the literature where the most stable perovskite is LaCoO<sub>3</sub>, the harder to reduce and the easily to oxidize [26,27].

Lanthanide oxides, e.g., sesquioxides and perovskites are basic and usually act as basic catalysts [28,29]. Lanthanide oxychlorides (LnOCl) catalyze some reactions that require basic catalysts, e.g., the oxidative coupling of methane [30–33]. However, various Lewis acidic catalysis based on lanthanide chlorides are known [34]. Therefore, it is expected that oxychlorides and to a lesser extent perovskites would provide the synergetic combination of the activation of CO<sub>2</sub> by the Lewis basic O<sup>2-</sup> sites and the activation of hydrogen by the Lewis acidic M<sup>3+</sup> (M = lanthanide or cobalt) sites indispensable for methanation of CO<sub>2</sub> [12,35].

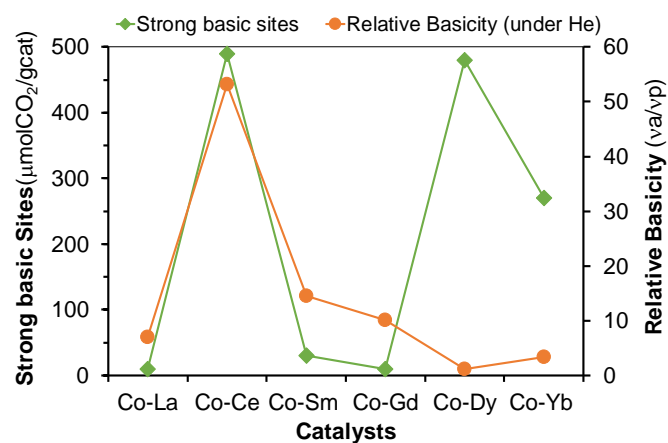
The importance cooperation between basic and acid sites is a known fact and it is very important to distinguish the catalysts acid-base properties. In this work, the acid-basic properties of the catalysts were studied by the absorption/desorption of CO<sub>2</sub> as a molecular probe (CO<sub>2</sub>-TPD) and by the study of their catalytic behavior in a model reaction, the dehydrogenation/dehydration of 2-propanol. The results obtained show that the catalysts obtained at 500 and 900 °C are basic (Tables S7 and S8), with a good correlation between the results obtained by the two techniques (Figure 5). Looking only at the relative basicity of the catalysts, it is possible to say that regardless of the calcination temperature, cerium catalysts are the most basic. Moreover, the basicity decreases along the lanthanide series for the aerogels calcined either at 500 or 900 °C, except for the ytterbium catalyst, which clearly show a contribution of either the lanthanide oxychlorides or perovskites for the catalyst's acid-base properties.

## 2.2. Hydrogenation of CO<sub>2</sub>

The results obtained with pure monometallic oxides of cerium and cobalt, which were also obtained by the epoxide addition method and calcined at 500 and 900 °C, confirm the positive effect obtained after addition of a rare earth to the catalysts. Figure 6 show such an effect in this case cerium using as example the cobalt-cerium bimetallic aerogels obtained in this work at two different temperatures. We can see that under the same conditions, pure cerium oxide catalyst is not active, while pure cobalt oxide catalyst deactivate markedly with the increase of the reaction temperature. In contrast, the cobalt-cerium bimetallic aerogels calcined at 500 and 900 °C not only does not deactivate, but on the contrary its activity increases with temperature and is significantly higher than that of pure cobalt oxide catalyst.



(a)



(b)

**Figure 5.** Acid-base properties of aerogels calcined at 500 °C (a) and at 900 °C (b) measured by CO<sub>2</sub>-TPD (strong basic sites) and dehydration/dehydrogenation of 2-propanol in inert atmosphere at 250 °C (relative basicity, va/vp; acetone/propene selectivity ratio).

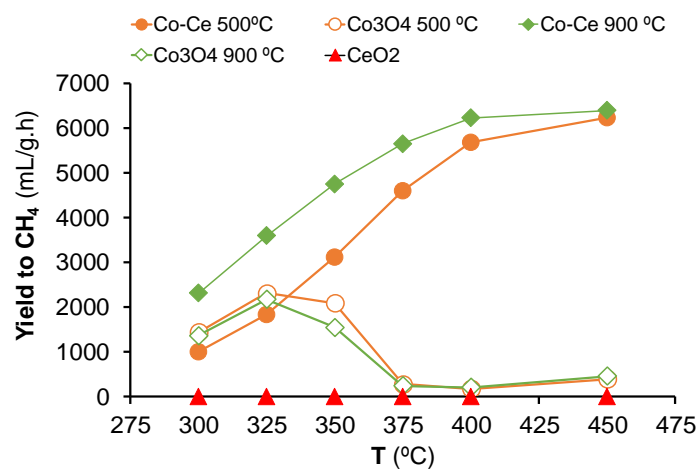
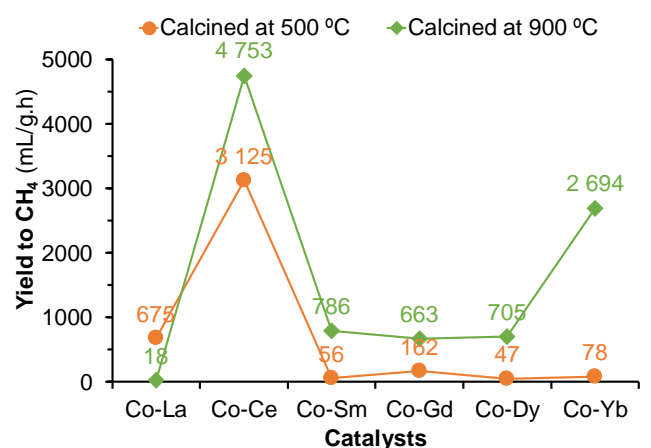
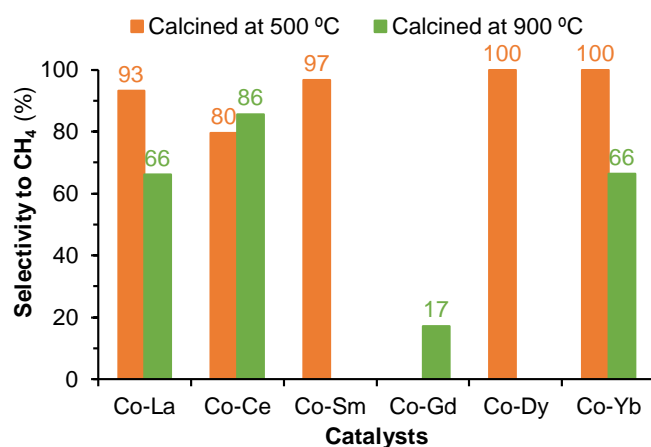


**Figure 6.** Addition of cerium to the cobalt catalyst and its effect on yield to CH<sub>4</sub> after pre-reduction under hydrogen (H<sub>2</sub>/CO<sub>2</sub> = 4, GHSV = 15,000 mL CO<sub>2</sub>/g<sub>cat</sub>·h).

Therefore, the presence of a rare earth plays an important role in the catalyst's activity for the methanation of CO<sub>2</sub>. Besides the presence of rare earths with different oxide phases (oxychlorides or perovskites) influence the nature of the active species for hydrogenation of CO<sub>2</sub> and consequently plays also an important role in their activity. Our results show that the cobalt-lanthanide aerogels calcined at 900 °C are generally more active but less selective for methane than the cobalt-lanthanide aerogels calcined at 500 °C with or without pre-reduction under hydrogen (Figure 7 and Figure S3, respectively).



(a)



(b)

**Figure 7.** Influence of the calcination temperature on the yield and selectivity to CH<sub>4</sub> ((a) and (b), respectively) obtained over pre-reduced samples (reaction temperature = 350 °C, H<sub>2</sub>/CO<sub>2</sub> = 4, GHSV = 15,000 mL CO<sub>2</sub>/g<sub>cat</sub>·h).

The catalyst's pre-reduction prior treatment to their test on the methanation of CO<sub>2</sub> is mentioned in the literature as indispensable for the formation of the dominant active species, in this case, metallic cobalt. The results obtained confirm, in almost all catalysts, that the pre-reduction of the bimetallic oxides increases their activity, regardless of the aerogels calcination temperature (Figure 8). The exceptions are the Co-Sm catalysts obtained after calcination at 500 °C and the Co-La catalyst obtained after calcination at 900 °C. In particular, the cobalt-lanthanum catalyst behavior can be explained by the fact that its pre-reduction requires a very high temperature (700 °C), which leads to an increase in particle size (sintering) and loss of active surface area due to sample sintering [36,37].

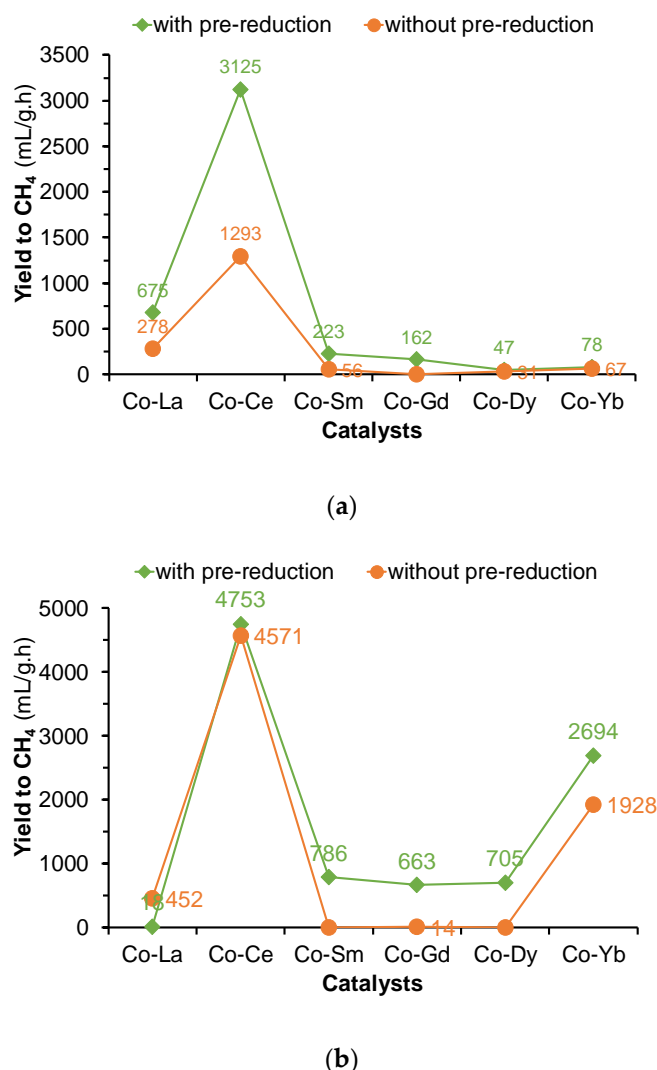
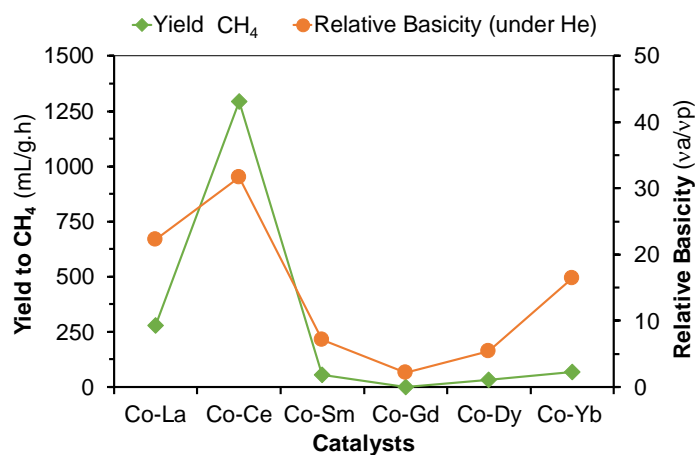
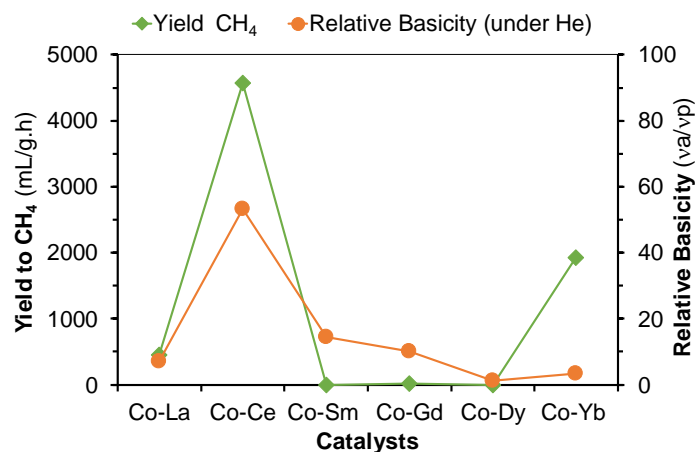


**Figure 8.** Effect of pre-reduction treatment on the activity of the aerogels calcined at 500 °C (a) and 900 °C (b) (reaction temperature = 350 °C, H<sub>2</sub>/CO<sub>2</sub> = 4, GHSV = 15,000 mL CO<sub>2</sub>/g<sub>cat</sub>.h).

It is also important to stress that the catalytic activity can be significantly influenced by some intrinsic properties such as the catalysts acid-base properties [29]. In this work, the results obtained show that regardless of the calcination temperature or the pre-reduction of the catalysts, the yield to methane increases with the catalysts basicity (Figure 9). The cobalt-cerium catalyst is clearly the most active (and the exception), but we have found that such influence varies throughout the lanthanide series, decreasing from lanthanum to ytterbium and following the basicity decreases along the lanthanide series described before. Moreover, the aerogels calcined at 900 °C (cobalt-lanthanide perovskites) are significantly more active than the aerogels calcined at 500 °C (cobalt-lanthanide oxychlorides) and we can draw a parallel with the higher basicity of the aerogels calcined at 900 °C. Additionally, the cobalt-perovskites are less selective than the cobalt-oxychloride catalysts (Figure S3), which can be attributed to the enhanced acidic character of the lanthanide oxychlorides and to a reinforced cooperative effect between basic and acidic sites.



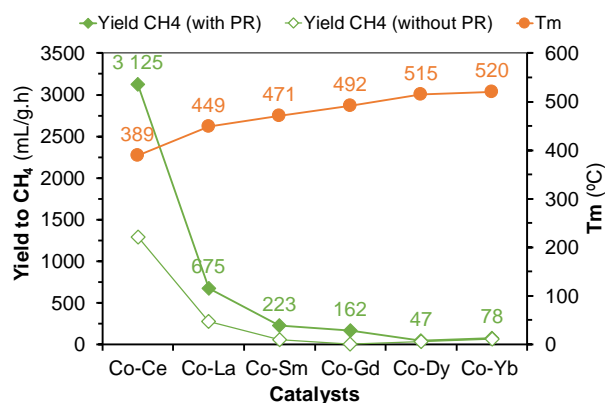
(a)



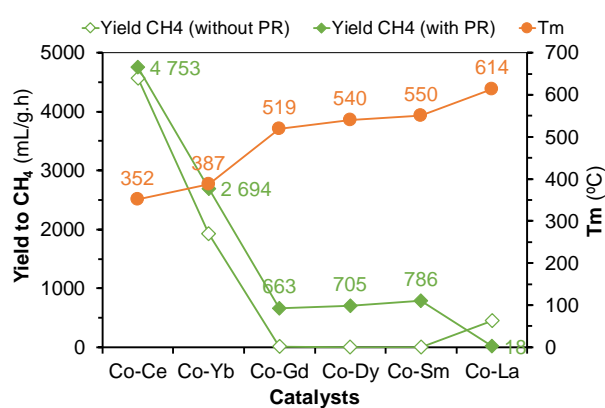
(b)

**Figure 9.** Correlation between yield to CH<sub>4</sub> at 350 °C and the relative basicity of bimetallic cobalt-lanthanide aerogels calcined at 500 °C (a) and 900 °C (b).

It was also observed that there is also an inverse correlation between catalyst activity and the temperatures at maximum reduction rate (H<sub>2</sub>-TPR; T<sub>m</sub>) measure before for both the type of samples: calcined at 500 °C or calcined at 900 °C (Figure 10). It is thus obvious that the presence of rare earth is not merely figurative and that there is a synergy between metals that explain the enhanced activity of cobalt after the addition of rare earths. Particularly for the samples pre-reduced under hydrogen where the presence of the rare earth could be more significant, preventing aggregation of metallic Co particles (sintering) and increasing the stability of the catalysts [5,9]. Therefore, it is not too much to stress the importance of the cooperative action of the lanthanide oxide phase on cobalt and the effect on the catalyst activity because if the main active specie is the metallic cobalt as shown by the analysis of the catalysts after reaction, taking into account that the amount of such specie at the surface is approximately the same for each type of catalysts, the presence and synergetic interaction with different lanthanide oxide phases will have repercussions on their properties, catalytic activity, and stability.



(a)



(b)

**Figure 10.** Influence of reduction temperature on the catalytic activity of bimetallic cobalt-lanthanide oxides calcined at 500 °C (a) and 900 °C (b); reaction temperature = 350 °C, GHSV = 15,000 mL/g<sub>cat</sub>·h and with pre-reduction.

On the other hand, parameters such as sintering or carbon deposition are those that normally lead to a marked deactivation of the catalysts. In this work, long-time stability tests were performed with the most active catalyst, the cerium catalyst obtained by calcination of the aerogel at 900 °C. The stability tests were performed with and without pre-reduction under hydrogen (Figure 11 and Figure S4, respectively). In both cases, the data obtained show that such catalyst is stable for at least 50 h (10 h at each temperature studied).

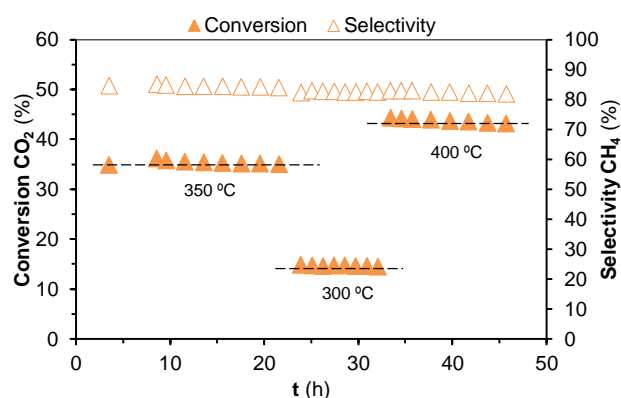


**Figure 11.** Stability of the bimetallic Co-Ce aerogel calcined at 900 °C, with pre-reduction, at different temperatures ( $H_2/CO_2 = 4$ , GHSV = 15,000 mL CO<sub>2</sub>/g<sub>cat</sub>·h).

Cobalt-based catalysts are known to be relatively resistant to thermal deactivation. Nevertheless, cobalt catalysts often suffer carbon deposition, changes in porosity and surface morphology, and in some cases, crystalline phase transformation may also occur, namely by reoxidation of cobalt particles leading to its deactivation [38,39], which was not the case of our catalysts and an important advantage.

Finally, two reference catalysts for the methanation of CO<sub>2</sub>, one commercial (Aldrich; 5%Rh/Al<sub>2</sub>O<sub>3</sub>) and other from the literature [21], described that one of the best (NiO/CeO<sub>2</sub>) were purchased (the first) or synthesized (the second) and tested under the same conditions as our best catalyst, the cobalt-cerium aerogel calcined at 900 °C and pre-reduced under hydrogen. The results obtained are unequivocal and show that although less selective, the methane yield obtained over our catalyst is comparable to those obtained over the two references, which is a good result and deserves to be stressed and reinforce the relevance of the catalysts preparation route that in this work, which shows cobalt-based catalysts as the best reported in the literature, regardless the nature of the active site (Table 1).

**Table 1.** Comparison of catalyst's activity.

Catalyst	Conversion CO <sub>2</sub> (%)	Yield CH <sub>4</sub> (%)	Selectivity CH <sub>4</sub> (%)
Co-Ce <sup>a,b</sup>	37.0	31.7	85.7
NiO/CeO <sub>2</sub> ref1 <sup>a,c</sup>	35.0	33.7	96.3
5%Rh/Al <sub>2</sub> O <sub>3</sub> ref2 <sup>a,d</sup>	35.6	35.5	99.8
Co-Ce <sup>e</sup>	26.1	24.9	95.3

<sup>a</sup> All catalysts were pre-treated under hydrogen (10%H<sub>2</sub> in He); 350 °C, P = 1; H<sub>2</sub>/CO<sub>2</sub> = 4, GHSV = 15,000 mL CO<sub>2</sub>/g<sub>cat</sub>.h. <sup>b</sup> Co-Ce aerogel calcined at 900 °C after pre-reduction under hydrogen (10% in He). <sup>c</sup> Synthesized as described in the literature [21]. <sup>d</sup> Commercial, purchased from Aldrich. <sup>e</sup> Experimental conditions: 200 °C, P = 5 bar, GHSV = 18,000 mL/g.h [12].

### 3. Materials and Methods

Cobalt-lanthanide aerogels (Co:Ln = 1; Ln = La, Ce, Sm, Gd, Dy, and Yb) were prepared by the epoxide addition method [22,40] using chlorides of the respective metals (Aldrich or Alpha Aesar; purity > 99%) as starting reagents. They were completely dissolved in absolute ethanol (Fischer Chemical, purity > 99.9%) at room temperature, followed by the addition of propylene oxide (Acros organics, 99.5%), the mixture stirred for further 5 min (molar ratio between metals and propylene oxide = 9), and the solution allowed to stand until complete gel formation. Then the gel obtained was aged in absolute ethanol for 48 h at 50 °C (sealed in the preparation vessel) and then dried by the organic solvent sublimation drying method (OSSD) [41] using successive mixtures of acetonitrile and ethanol (50, 80, and 100% (v/v), respectively) for periods of 24 h at each concentration and at 50 °C. As an example, for the preparation of Co-Ce aerogel 1.177 g (3 mmol) of CeCl<sub>3</sub>·7H<sub>2</sub>O (Aldrich chemistry, 99%) and 0.7138 g (3 mmol) of CoCl<sub>2</sub>·6H<sub>2</sub>O (Alpha Aesar, 99%) were dissolved in 6.3 mL of absolute ethanol and subsequently 3.86 mL (55 mmol) of propylene oxide were added, the solution stirred until gel formation and finally dried using 10–15 mL portions of the acetonitrile/ethanol mixtures. Finally, aiming the synthesis of bimetallic oxides, the aerogels were calcined at 500 and 900 °C under air, at a heating rate of 1 °C/min during 2 h. In the end, the product is crushed, and the particle size reduced to 200 mesh (75 µm).

The crystalline structure of the catalysts was analyzed by X-ray diffraction (powder) and recorded on a Bruker D8 advance diffractometer (Cu, Kα monochromatic radiation, λ = 1.5406 Å). The operational settings for all scans were voltage = 40 kV; current = 30 mA; 2θ scan range 19–81° using a step size of 0.03° at a time per step 0.5 s. For identification purposes, the relative intensities (I/I<sub>0</sub>) and the d-spacing (Å) were compared with standard JCPDS powder diffraction files [42]. The particle size was determined by means of the Scherer's equation.

Surface morphology was analyzed by SEM using a FE-SEM JEOL JSM-6500F (Peabody, MA, USA), operating at 15–20 keV and 80 A. The surface chemical composition was determined by EDS using a B-U Bruker Quantax 400 EDS system (Billica, MA, USA), installed in Microlab on Instituto Superior Técnico, Lisbon. Specific surface areas (BET method; single point relative pressure P/P<sub>0</sub> = 0.3, flow 20 mL/min

using a mixture of 30% nitrogen in helium) were measured on a Micromeritics ChemSorb 2720 instrument (Norcross, GA, USA). BET surface areas of all catalysts are listed in Table S1.

The reducibility of the bimetallic oxides was studied by temperature programmed reduction under hydrogen ( $H_2$ -TPR) and performed on a Micromeritics ChemSorb 2720 instrument. The samples were placed in a specific Micromeritics quartz type U reactor and reduced under a 10% $H_2$ /argon mixture (20–1000 °C, at 10 °C/min, flow 20 mL/min). Quantitative  $H_2$ -uptakes were evaluated by integration of the experimental  $H_2$ -TPR curves, based on previous calibration measurements with NiO powders (Aldrich, 99.99995% purity). The optimized profile resolution was obtained by judicious choice of the sample weight, around 15 mg of each sample.

The acid-base properties of the catalysts were evaluated by studying its behavior on a model reaction: the dehydrogenation/dehydration of 2-propanol. These tests were carried out in a Fixed-bed U-shaped Pyrex reactor (inside volume of 15 mL) and studied in the temperature range 175 to 250 °C, at atmospheric pressure using a 0.25% (*v/v*%) mixture of 2-propanol in air ( $N_2/O_2$ :80/20 *v/v*, Air Liquide K, purity 99.9995%) with a GHSV of 1007 mL/ $g_{\text{catalyst}} \cdot h$ . The reactor outlet gas composition was analyzed online by gas chromatography using an Agilent 7280D chromatograph equipped with a flame ionization detector (FID) and a capillary column HP\_PLOT\_U, L = 30 m, ID = 0.32 mm. Relative basicity was defined as the ratio between the selectivity to acetone (basic sites) and propene (acid sites),  $v_A/v_P$ .

Catalytic tests for the hydrogenation of  $CO_2$  were carried out in U-shaped Pyrex fixed bed (porous plate) plug-flow reactors with an internal volume of  $\approx 7$  mL. Catalyst grain size was controlled using a 200 Mesh sieve (0.075 mm),  $m = 10$ –30 mg (max. 1 mm bed thickness). Mass flow controllers (Aalborg series A) were used to control  $CO_2$ ,  $H_2$ , and He flows. A gaseous mixture of  $CO_2 / H_2$  (1:4 mol/mol) was used and the reaction studied with an adequate Gas Hourly Space Velocity (GHSV, 15,000 mL of  $CO_2$  per g of catalyst and per h). All tests were performed at atmospheric pressure and the effect of the reaction temperatures studied between 250 to 450 °C. The amount of catalyst was selected in such a way that rate limitation by external mass and heat transport processes under differential conditions proved to be negligible by applying suitable experimental criteria, such as those defined by Mears ( $-r_0Rn/kC \ll 0.15$ ) [43,44], Froment and Bischoff ( $\Delta PCH_4 \ll 1 \times 10^{-4}$  atm;  $\Delta T$  max  $\ll 1$  K) [45] or Weiz/Prater ( $R^2r/CsDe \ll 0.3$ ) [44]. Moreover, to study the effect of a pre-reduction on the catalytic behavior, all aerogels calcined at 500 °C were submitted to a pre-treatment under hydrogen (10%  $H_2$  in He) at 500 °C for 30 min (10 °C/m in heating rate), whereas those calcined at 900 °C were pre-reduced between 400 and 700 °C, adjusted by  $H_2$ -TPR profiles (Co-La 700 °C, Co-Ce 400 °C, Co-Sm, Co-Gd, and Co-Dy 600 °C, and Co-Yb 450 °C).

The reactor outlet gas composition was analyzed online by gas chromatography using an Agilent 4890D GC equipped with a thermal conductivity detector (TCD) and a Restek ShinCarbon ST column (L = 2.0 m, 1/8 in., ID = 1 mm, 100/200 mesh) for the detection of all gaseous reagents and products. GC system uses a 6-port gas-sampling valve with a 0.250 mL loop for online analysis. Before analysis, the outlet gas was cooled in an ice-water trap in order to avoid column contamination, namely by water (not detected). Unless stated otherwise, all pure gases and mixtures were purchased from Air Liquide and supplied with an Alphagaz 2 purity. The values reported in this paper represent the steady state activities after 1 h on stream.

Catalysts activity was defined as the volume of  $CH_4$  converted per g of catalyst per hour ( $mL_{CH_4} g^{-1} h^{-1}$ ). The conversion of  $CO_2$  and selectivity to  $CH_4$  and CO were calculated as follows: Conv.  $CO_2$  (%) =  $([CH_4]_o + [CO]_o)/([CO]_o + [CH_4]_o + [CO_2]_i) \times 100$ ; Sel.  $CH_4$  (%) =  $[CH_4]_o/([CO]_o + [CH_4]_o) \times 100$ ; Sel.CO (%) =  $[CO]_o/([CO]_o + [CH_4]_o) \times 100$ , where  $[CO_2]_i$  is the inlet flow rate of  $CO_2$  and  $[CO_2]_o$ ,  $[CH_4]_o$  and  $[CO]_o$  are the outlet flow rates of  $CO_2$ ,  $CH_4$  and CO. Detector calibration was performed using external reference mixtures containing all reagents ( $H_2$ ,  $CO_2$ ) and all expected products ( $CH_4$ , CO,  $C_2H_2$ ,  $C_2H_4$ ,  $C_2H_6$ ,  $C_3H_8$ ). The confidence level was better than 95%. For comparison purposes, a commercial rhodium catalyst supported on alumina (Aldrich, 5 wt.%) was used as received.

#### 4. Conclusions

Cobalt-lanthanide aerogels (Co-Ln, Ln = La, Ce, Sm, Gd, Dy, and Yb; Co/Ln = 1) were obtained by the epoxide addition method and its calcination at different temperatures led to the formation of distinct oxide phases: oxychlorides, in the case of calcination at 500 °C ( $\text{Co}_3\text{O}_4 \cdot 3\text{LnOCl}$ ; Ln = La, Sm, Gd, Dy, and Yb) and perovskites, in the case of calcination at 900 °C ( $\text{LnCoO}_3$ ; Ln = La, Sm, Gd, and Dy) that coexist in synergetic interaction with cobalt. In both cases, the exceptions were the cerium and ytterbium catalysts that stabilize as sesquioxides,  $\text{Co}_3\text{O}_4 \cdot 3\text{CeO}_2$  (at 500 °C and 900 °C) or  $2\text{Co}_3\text{O}_4 \cdot 3\text{Yb}_2\text{O}_3$  (at 900 °C), respectively.

The catalytic proprieties were evaluated for the methanation of  $\text{CO}_2$  and we have found that rare earth oxychlorides and perovskites have a marked influence on the catalytic behavior of the cobalt-lanthanide aerogels calcined at 500 or 900 °C, whose intrinsic properties such as the basicity or oxygen lability significantly influence their catalytic activity for methanation of  $\text{CO}_2$ . In fact, the more basic and the more labile oxygen, the more active were the catalysts, which sanction the potential synergetic effect between cobalt and rare earth.

The cobalt-lanthanide aerogels also proved to be very stable, during at least 80 h of reaction and among them, the catalysts calcined at 500 °C are the most stable and the most promising despite being less active than the catalysts calcined at 900 °C. Briefly, the cobalt-rare-earth catalysts developed in this work proved to be active, selective, and stable for the methanation of  $\text{CO}_2$ , and despite the fact that they are not the most active among the catalysts reported in the literature, they seem clearly to be an alternative to be considered for future developments in this area of knowledge.

**Supplementary Materials:** The following are available online at <http://www.mdpi.com/2073-4344/10/6/704/s1>, Table S1: Surface area of the aerogels as prepared and after calcination treatment, Table S2: EDS analysis of cobalt-lanthanide aerogels calcined at 500 °C, Table S3: EDS analysis of cobalt-lanthanide aerogels calcined at 900 °C, Table S4: Estimated cobalt particles size of cobalt-lanthanide aerogels calcined at 500 °C and 900 °C, Table S5:  $\text{H}_2$ -TPR consumption of hydrogen obtained and expected for the aerogels calcined at 500 °C, Table S6:  $\text{H}_2$ -TPR consumption of hydrogen obtained and expected for the aerogels calcined at 900 °C, Table S7: Dehydrogenation/dehydration of 2-propanol over cobalt-lanthanide aerogels calcined at 500 °C, at 250 °C under oxidative atmosphere (between parentheses under inert atmosphere), Table S8: Dehydrogenation/dehydration of 2-propanol over cobalt-lanthanide aerogels calcined at 900 °C, at 250 °C under oxidative atmosphere (between parentheses under inert atmosphere), Figure S1: SEM images of the aerogels calcined at 500: Co-La (a), Co-Ce (b), Co-Sm (c); Co-Gd (d), Co-Dy (e) and Co-Yb (f), Figure S2: SEM images of the aerogels calcined at 900 °C: Co-La (a), Co-Ce (b), Co-Sm (c); Co-Gd (d), Co-Dy (e) and Co-Yb (f), Figure S3: Temperature effect on yield and selectivity to methane of the cobalt-lanthanide aerogels calcined at 500 °C (a,b) and at 900 °C (c,d), Figure S4: Stability of the bimetallic Co-Ce aerogel calcined at 900 °C, without pre-reduction, at different temperatures ( $\text{H}_2/\text{CO}_2 = 4$ , GHSV = 15,000 mL  $\text{CO}_2/\text{g}_{\text{cat}} \cdot \text{h}$ ).

**Author Contributions:** Conceptualization, J.B.B. and A.C.F.; data curation, R.P.d.S.; formal analysis, J.B.B., R.P.d.S. and A.C.F.; funding acquisition, A.C.F.; investigation, J.B.B., R.P.d.S. and A.C.F.; methodology, J.B.B. and A.C.F.; project administration, A.C.F.; resources, J.B.B.; supervision, J.B.B. and A.C.F.; writing—original draft, J.B.B.; writing—review and editing, J.B.B. and A.C.F. All authors have read and agreed to the published version of the manuscript.

**Funding:** This research was funded by Portuguese “Fundação para a Ciência e Tecnologia”, FCT, through the PTDC/EAM-PEC/28374/2017 and UID/Multi/04349/2019 project.

**Conflicts of Interest:** The authors declare no conflicts of interest.

#### References

1. Li, W.H.; Wang, H.Z.; Jiang, X.; Zhu, J.; Liu, Z.M.; Guo, X.W.; Song, C.S. A short review of recent advances in  $\text{CO}_2$  hydrogenation to hydrocarbons over heterogeneous catalysts. *RSC Adv.* **2018**, *8*, 7651–7669. [[CrossRef](#)]
2. Bui, M.; Adjiman, C.S.; Bardow, A.; Anthony, E.J.; Boston, A.; Brown, S.; Fennell, P.S.; Fuss, S.; Galindo, A.; Hackett, L.A.; et al. Carbon capture and storage (CCS): The way forward. *Energy Environ. Sci.* **2018**, *11*, 1062–1176. [[CrossRef](#)]
3. Sanz-Perez, E.S.; Murdock, C.R.; Didas, S.A.; Jones, C.W. Direct capture of  $\text{CO}_2$  from ambient air. *Chem. Rev.* **2016**, *116*, 11840–11876. [[CrossRef](#)] [[PubMed](#)]

4. Ronsch, S.; Schneider, J.; Matthischke, S.; Schluter, M.; Gotz, M.; Lefebvre, J.; Prabhakaran, P.; Bajohr, S. Review on methanation—From fundamentals to current projects. *Fuel* **2016**, *166*, 276–296. [[CrossRef](#)]
5. Frontera, P.; Macario, A.; Ferraro, M.; Antonucci, P. Supported catalysts for CO<sub>2</sub> methanation: A review. *Catalysts* **2017**, *7*, 59. [[CrossRef](#)]
6. Zheng, J.; Wang, C.Y.; Chu, W.; Zhou, Y.L.; Kohler, K. CO<sub>2</sub> methanation over supported Ru/Al<sub>2</sub>O<sub>3</sub> catalysts: Mechanistic studies by in situ infrared spectroscopy. *Chemistryselect* **2016**, *1*, 3197–3203. [[CrossRef](#)]
7. Riedel, T.; Claeys, M.; Schulz, H.; Schaub, G.; Nam, S.S.; Jun, K.W.; Choi, M.J.; Kishan, G.; Lee, K.W. Comparative study of Fischer-Tropsch synthesis with H<sub>2</sub>/CO and H<sub>2</sub>/CO<sub>2</sub> syngas using Fe- and Co-based catalysts. *Appl. Catal. A Gen.* **1999**, *186*, 201–213. [[CrossRef](#)]
8. Dorner, R.W.; Hardy, D.R.; Williams, F.W.; Davis, B.H.; Willauer, H.D. Influence of Gas Feed Composition and Pressure on the Catalytic Conversion of CO<sub>2</sub> to Hydrocarbons using a traditional cobalt-based fischer-tropsch catalyst. *Energy Fuels* **2009**, *23*, 4190–4195. [[CrossRef](#)]
9. Zhang, J.L.; Su, X.J.; Wang, X.; Ma, Q.X.; Fan, S.B.; Zhao, T.S. Promotion effects of Ce added Fe-Zr-K on CO<sub>2</sub> hydrogenation to light olefins. *React. Kinet. Mech. Cat.* **2018**, *124*, 575–585. [[CrossRef](#)]
10. Zeng, S.H.; Du, Y.; Su, H.Q.; Zhang, Y.L. Promotion effect of single or mixed rare earths on cobalt-based catalysts for Fischer-Tropsch synthesis. *Catal. Commun.* **2011**, *13*, 6–9. [[CrossRef](#)]
11. Le, T.A.; Kim, M.S.; Lee, S.H.; Park, E.D. CO and CO<sub>2</sub> methanation over supported cobalt catalysts. *Top. Catal.* **2017**, *60*, 714–720. [[CrossRef](#)]
12. Zhou, Y.W.; Jiang, Y.X.; Qin, Z.Z.; Xie, Q.R.; Ji, H.B. Influence of Zr, Ce, and La on Co<sub>3</sub>O<sub>4</sub> catalyst for CO<sub>2</sub> methanation at low temperature. *Chin. J. Chem. Eng.* **2018**, *26*, 768–774. [[CrossRef](#)]
13. Ferreira, A.C.; Ferraria, A.M.; do Rego, A.M.B.; Goncalves, A.P.; Correia, M.R.; Gasche, T.A.; Branco, J.B. Partial oxidation of methane over bimetallic nickel-lanthanide oxides. *J. Alloys Compd.* **2010**, *489*, 316–323. [[CrossRef](#)]
14. Ferreira, A.C.; Ferraria, A.M.; do Rego, A.M.B.; Goncalves, A.P.; Girao, A.V.; Correia, R.; Gasche, T.A.; Branco, J.B. Partial oxidation of methane over bimetallic copper-cerium oxide catalysts. *J. Mol. Catal. A Chem.* **2010**, *320*, 47–55. [[CrossRef](#)]
15. Ferreira, A.C.; Goncalves, A.P.; Gasche, T.A.; Ferraria, A.M.; do Rego, A.M.B.; Correia, M.R.; Bola, A.M.; Branco, J.B. Partial oxidation of methane over bimetallic copper- and nickel-actinide oxides (Th, U). *J. Alloys Compd.* **2010**, *497*, 249–258. [[CrossRef](#)]
16. Branco, J.B.; Ferreira, A.C.; Gasche, T.A.; Pimenta, G.; Leal, J.P. Low temperature partial oxidation of methane over bimetallic nickel-f block element oxide nanocatalysts. *Adv. Synth. Catal.* **2014**, *356*, 3048–3058. [[CrossRef](#)]
17. Branco, J.B.; Ferreira, A.C.; Leal, J.P. Light hydrocarbons production over bimetallic calcium-actinide oxide catalysts using N<sub>2</sub>O as oxidant. *J. Mol. Catal. A Chem.* **2014**, *390*, 45–51. [[CrossRef](#)]
18. Ferreira, A.C.; Gasche, T.A.; Leal, J.P.; Branco, J.B. Methane activation with nitrous oxide over bimetallic oxide Ca-lanthanide nanocatalysts. *Mol. Catal.* **2017**, *443*, 155–164. [[CrossRef](#)]
19. Branco, J.B.; Ferreira, A.C. Methanation of CO<sub>2</sub> over bimetallic Ni-5f block element (Th, U) oxides. *Eur. J. Inorg. Chem.* **2019**, 1039–1045. [[CrossRef](#)]
20. Ferreira, A.C.; Branco, J.B. Methanation of CO<sub>2</sub> over nanostructured nickel-4f block element bimetallic oxides. *Int. J. Hydrog. Energy* **2019**, *44*, 6505–6513. [[CrossRef](#)]
21. Zhou, G.L.; Liu, H.R.; Cui, K.K.; Xie, H.M.; Jiao, Z.J.; Zhang, G.Z.; Xiong, K.; Zheng, X.X. Methanation of carbon dioxide over Ni/CeO<sub>2</sub> catalysts: Effects of support CeO<sub>2</sub> structure. *Int. J. Hydrog. Energy* **2017**, *42*, 16108–16117. [[CrossRef](#)]
22. Clapsaddle, B.J.; Neumann, B.; Wittstock, A.; Sprehn, D.W.; Gash, A.E.; Satcher, J.H.; Simpson, R.L.; Baumer, M. A sol-gel methodology for the preparation of lanthanide-oxide aerogels: Preparation and characterization. *J. Solgel Sci. Technol.* **2012**, *64*, 381–389. [[CrossRef](#)]
23. Cho, Y.J.; Yang, H.C.; Eun, H.C.; Kim, E.H.; Kim, I.T. Characteristics of oxidation reaction of rare-earth chlorides for precipitation in LiCl-KCl molten salt by oxygen sparging. *J. Nucl. Sci. Technol.* **2006**, *43*, 1280–1286. [[CrossRef](#)]
24. Ben Farhat, L.; Ben Hassen, R.; Dammak, L. Rietveld refinement of YbCoO<sub>3</sub> prepared from aqueous solution-gel precursor. *Powder Diffr.* **2007**, *22*, 35–39. [[CrossRef](#)]

25. Zhang, X.J.; Zhao, M.; Song, Z.X.; Zhao, H.; Liu, W.; Zhao, J.G.; Ma, Z.A.; Xing, Y. The effect of different metal oxides on the catalytic activity of a  $\text{Co}_3\text{O}_4$  catalyst for toluene combustion: Importance of the structure-property relationship and surface active species. *New J. Chem.* **2019**, *43*, 10868–10877. [[CrossRef](#)]
26. Lago, R.; Bini, G.; Pena, M.A.; Fierro, J.L.G. Partial oxidation of methane to synthesis gas using  $\text{LnCoO}_3$  perovskites as catalyst precursors. *J. Catal.* **1997**, *167*, 198–209. [[CrossRef](#)]
27. Arakawa, T.; Ohara, N.; Shiokawa, J. Reduction of Perovskite Oxide  $\text{La-EuCoO}_3$  in a Hydrogen Atmosphere. *J. Mater. Sci.* **1986**, *21*, 1824–1827. [[CrossRef](#)]
28. Hattori, H. Heterogeneous Basic Catalysis. *Chem. Rev.* **1995**, *95*, 537–558. [[CrossRef](#)]
29. Tanabe, K.; Misono, M.; Ono, Y.; Hattori, H. *New Acids and Bases-Their catalytic Properties*; Studies in Surface Science and Catalysis; Delmon, B., Yates, J.T., Eds.; Elsevier: Amsterdam, The Netherlands, 1989; Volume 51, pp. 200–211.
30. Williams, J.; Jones, R.H.; Thomas, J.M.; Kent, J. A comparison of the catalytic performance of the layered oxychlorides of bismuth, lanthanum and samarium in the conversion of methane to ethylene. *Catal. Lett.* **1989**, *3*, 247–255. [[CrossRef](#)]
31. Ueda, W.; Sakyu, F.; Isozaki, T.; Morikawa, Y.; Thomas, J.M. Catalytic oxidative dimerization of methane to form  $\text{C}_2$ -Compounds over Arppe phase oxychlorides of Bi, La and Sm. *Catal. Lett.* **1991**, *10*, 83–90. [[CrossRef](#)]
32. Chanaud, P.; Julbe, A.; Larbot, A.; Guizard, C.; Cot, L.; Borges, H.; Fendler, A.G.; Mirodatos, C. Catalytic membrane reactor for oxidative coupling of methane. 1. preparation and characterization of  $\text{LaOCl}$  membranes. *Catal. Today* **1995**, *25*, 225–230. [[CrossRef](#)]
33. Kienneman, A.; Kieffer, R.; Kaddouri, A.; Poix, P.; Rehspringer, J.L. Oxidative coupling of methane over  $\text{LnLiO}_2$ ,  $\text{LnNaO}_2$  and  $\text{LnO}_x$  catalysts ( $\text{Ln} = \text{Sm, Nd, La}$ ;  $X = \text{Cl, Br}$ ). Promoting effect of  $\text{MgO}$ ,  $\text{CaO}$  and  $\text{SrO}$ . *Catal. Today* **1990**, *6*, 409–416. [[CrossRef](#)]
34. Molander, G.A. Application of lanthanide reagents in organic-synthesis. *Chem. Rev.* **1992**, *92*, 29–68. [[CrossRef](#)]
35. Yasuda, H.; He, L.N.; Sakakura, T. Cyclic carbonate synthesis from supercritical carbon dioxide and epoxide over lanthanide oxychloride. *J. Catal.* **2002**, *209*, 547–550. [[CrossRef](#)]
36. Xu, J.H.; Su, X.; Duan, H.M.; Hou, B.L.; Lin, Q.Q.; Liu, X.Y.; Pan, X.L.; Pei, G.X.; Geng, H.R.; Huang, Y.Q.; et al. Influence of pretreatment temperature on catalytic performance of rutile  $\text{TiO}_2$ -supported ruthenium catalyst in  $\text{CO}_2$  methanation. *J. Catal.* **2016**, *333*, 227–237. [[CrossRef](#)]
37. Tada, S.; Kikuchi, R.; Urasaki, K.; Satokawa, S. Effect of reduction pretreatment and support materials on selective  $\text{CO}$  methanation over supported Ru catalysts. *Appl. Catal. A Gen.* **2011**, *404*, 149–154. [[CrossRef](#)]
38. Ahn, C.I.; Koo, H.M.; Jin, M.; Kim, J.M.; Kim, T.; Suh, Y.W.; Yoon, K.J.; Bae, J.W. Catalyst deactivation by carbon formation during  $\text{CO}$  hydrogenation to hydrocarbons on mesoporous  $\text{Co}_3\text{O}_4$ . *Microporous Mesoporous Mater.* **2014**, *188*, 196–202. [[CrossRef](#)]
39. Khodakov, A.Y.; Chu, W.; Fongarland, P. Advances in the development of novel cobalt Fischer-Tropsch catalysts for synthesis of long-chain hydrocarbons and clean fuels. *Chem. Rev.* **2007**, *107*, 1692–1744. [[CrossRef](#)]
40. Wei, T.Y.; Chen, C.H.; Chang, K.H.; Lu, S.Y.; Hu, C.C. Cobalt oxide aerogels of ideal supercapacitive properties prepared with an epoxide synthetic route. *Chem. Mater.* **2009**, *21*, 3228–3233. [[CrossRef](#)]
41. Ren, L.L.; Cui, S.M.; Cao, F.C.; Guo, Q.H. An easy way to prepare monolithic inorganic oxide aerogels. *Angew. Chem. Int. Ed.* **2014**, *53*, 10147–10149. [[CrossRef](#)]
42. JCPDS. *The Powder Diffraction File*; JCPDS: Swarthmore, PA, USA, 1981.
43. Dekker, F.H.M.; Bliet, A.; Kapteijn, F.; Moulijn, J.A. Analysis of mass and heat transfer in transient experiments over heterogeneous catalysts. *Chem. Eng. Sci.* **1995**, *50*, 3573–3580. [[CrossRef](#)]
44. Oyama, S.T.; Zhang, X.; Lu, J.; Gu, Y.; Fujitani, T. Epoxidation of propylene with  $\text{H}_2$  and  $\text{O}_2$  in the explosive regime in a packed-bed catalytic membrane reactor. *J. Catal.* **2008**, *257*, 1–4. [[CrossRef](#)]
45. Froment, G.F.; Bischoff, K.B.; De Wilde, J. *Chemical Reactor Analysis and Design*; John Wiley & Sons: Hoboken, NJ, USA, 1979.

